# Dalton Transactions

Accepted Manuscript






ROYAL SOCIETY OF CHEMISTRY

www.rsc.org/dalton

# Exploring the Mechanism of Grignard Methathesis Polymerization of 3-alkylthiophenes

**Naeimeh Bahri-Laleh,[1]* Albert Poater,[2] Luigi Cavallo,[3] and Seyed Amin Mirmohammadi[1]**

[1]*Department of Polymerization Engineering, Iran Polymer and Petrochemical Institute, P.O. Box 14965/115, Tehran, Iran.* [2]*Institut de Química Computacional i Catàlisi and Departament de Química, Universitat de Girona, Campus Montilivi, 17071 Girona, Catalonia, Spain.* [3]*Department of Chemistry, University of Salerno, Via Ponte don Melillo, Fisciano I-84084, Italy.*

**To whom correspondence should be addressed**: n.bahri@ippi.ac.ir, Tel: +982148662339, Fax: +982144196583.

## Abstract

In this study we have investigated computationally the mechanism of polymerization of 2,5-dibromo 3-butylthiophene via GRIM method, with a focus on the origin of the Head to Tail (HT) selectivity. To this end, first Grignard reagent underwent oxidative addition to monomer to afford the 2-bromo-5-chloromagnesio-3-butylthiophene (intermediate **I1**) or the 2-chloromagnesio 5-bromo-3-butylthiophene (intermediate **I2**) regioisomers. Then intermediates **I1** and **I2** were polymerized catalytically to a series of regiospecific poly-3-butylthiophenes using the commonly used Ni(dppp)$Cl_2$ [dppp: 1,3-bis(diphenylphosphino) propane] and Pd(dppp)$Cl_2$ catalysts. Due to asymmetric nature of **I1** and **I2** that act as the active monomeric species, 6 coupling modes may occur. The whole energy profile of all modes has been studied by considering a three stages mechanism, including coordination, transmetalation, and reductive elimination, to compare quantitatively the ability of so called catalysts in selective coupling of

desired isomers to produce regioregular poly3-butylthiophene. Finally, to quantify the steric role of the dppp in regioselectivity, analysis of the buried volume in terms of steric maps was employed.

**Keywords:** DFT calculations, GRIM, poly(3-alkylthiophene) (P3AT), regularity, Grignard, Solar cell.

## 1. Introduction

Regioregular poly(3-alkylthiophene) (P3AT) has received much attention in recent years because of its small band gap, high electrical conductivity, and interesting properties such as light emitting ability and high field effect mobility.[1,2] In P3ATs the incorporation of the alkyl substituent can occur in three different patterns on each bithiophene unit. The substituents can be located on the 2 and 5', the 2 and 2', or the 5 and 5' sites (see Scheme 1). The most common way to describe the 3-alkythiophene couplings is by denominating the sterically crowded 2-position as the ‘‘head’’ and 5-position as the ‘‘tail’’. So, substitution patterns with 2,2' substituents have been termed head-to-head (HH) linkages, patterns with 2,5' substitution are head-to-tail (HT) linkages, and patterns with 5,5' substitution are tail-to-tail (TT) linkages.

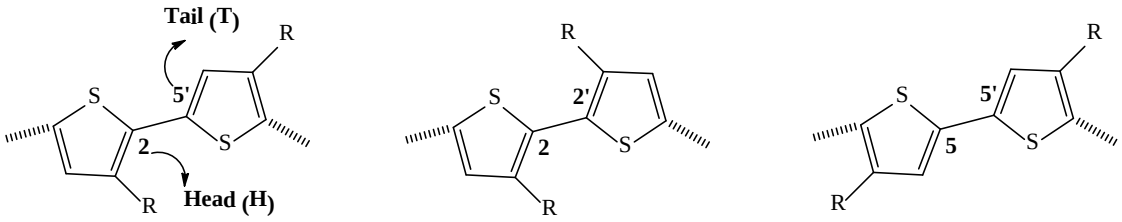

**Scheme 1**

In each bithiophene unit, thiophene rings can be located in the syn or anti position (see Schemes 2 and 3). Therefore, introducing 3-alkylthiophene monomers with comparable reactivity implies the necessity of considering six different reaction mechanisms of cross coupling.

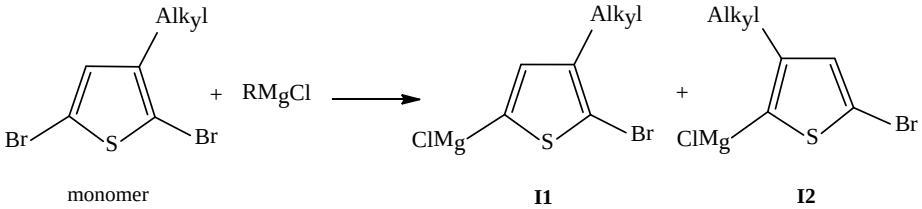


**Scheme 2**

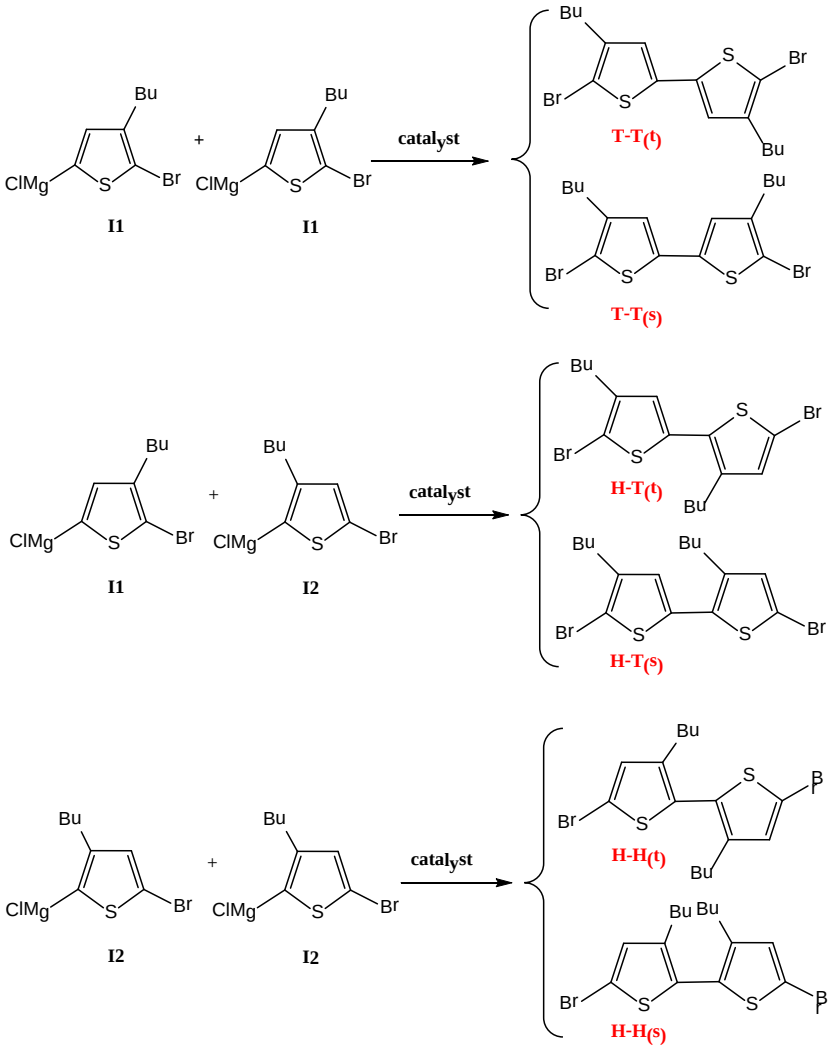

**Scheme 3**

The physical properties of P3ATs can be altered by varying the substitution pattern of the substituent along the polymer chain.[3] The HT linkages have smaller steric interactions and result in P3ATs with superior electronic properties, whereas the HH linkages have greater steric interactions and provide P3ATs with less extended conjugation.[4] Many of the recent synthetic investigations of P3ATs have focused on the development of HT regiospecific polymers due to the preferential electrical conductivities and optical nonlinearity.[5-7]

Structurally homogeneous PATs, denoted as regioregular PATs (rrPAT), can be obtained by one of three general strategies.[8] the McCullough method,[9] the Rieke method[10] or the GRIM (Grignard metathesis) method.[11] One strong advantage of the GRIM method is that the use of both cryogenic temperatures and highly reactive metals, which are basic conditions in the McCullough and Rieke methods, is unnecessary. Consequently, it offers a quick and easy preparation of rrP3ATs and enables the production of kilogram scale high molecular weight rrP3ATs. In this method, 2,5-dibromo-3-alkylthiophene is treated with 1 equiv of any Grignard reagent (RMgX) to form a mixture of intermediates **I1** and **I2** in a ratio from 85:15 to 75:25 (see Scheme 2).

Then, upon addition of Ni or Pd type catalysts, rrP3ATs with high regularity and desired molecular weight are obtained.

It has been shown, in the catalytic synthesis of HT-P3ATs, that the choice of the catalyst is critical in determining the % HT couplings in the resultant polymer. Catalysts with sterically demanding ligands (like dppe (bis(diphenylphosphino)ethane) and dppp (bis(diphenylphosphino)propane)) and small metal centers like Ni afford P3ATs with a high

degree of regioselectivity (>98.5% HT couplings). Less bulky, labile ligands like $PPh_3$ combined with larger metal centers like Pd lead to a regiorandom sample of P3ATs.[5]

Although extensive experimental studies on GRIM polymerization of 2,5-dibromo-3-alkylthiophenes have been made to unravel the basic mechanisms in the catalytic process, due to the nature of polymerizations, the direct observation of mechanism in situ is difficult and the present results do not fully explain the regioselectivity of the polymerization.[12] On the other hand, no efforts have been performed from a theoretical point of view to shed light on solving or improving these issues.

For this reason, we decided to investigate computationally the head to tail selectivity of the most well known polymerization catalysts, Ni(dppp)$Cl_2$ and Pd(dppp)$Cl_2$, using 2,5-dibromo-3-butylthiophene as a model monomer to get a reasonable overview of the polymerization steps. To this end, energy profile of all the 6 coupling modes in Scheme 2 has been studied by considering a three stages mechanism, including coordination (or oxidative addition), transmetalation, and reductive elimination, to compare quantitatively the ability of so called catalysts in regioregular synthesis of P3ATs.

## 2. Computational Details

The DFT calculations were performed with the Gaussian03 package,[13] using the B3LYP hybrid GGA functional of Becke-Lee, Parr, and Yang.[14,15] In all cases the electronic configuration of the molecular systems was described with the standard split valence basis set with a polarization function of Ahlrichs and co-workers for H, C, P, S, Br and Cl (SVP keyword in Gaussian09).[16] For Ni and Pd we used the small-core, quasi-relativistic Stuttgart/Dresden effective core potential, with an associated valence basis set (SDD keywords in Gaussian09).[17]

For all the computed species the singlet is the electronic ground state and thus closed shell calculations were performed. Characterization of the located stationary points as minima or transition state was performed by frequency calculations. Total energies and optimized geometries are provided in the Supporting Information.

The buried volume calculations were performed with the Samb*V*ca. package developed by Cavallo et al.[18] The radius of the sphere around the metal center was set to 3.5 Å, while for the atoms we adopted the Bondi radii scaled by 1.17, and a mesh of 0.1 Å was used to scan the sphere for buried voxels. The steric maps were evaluated with a modified version of the Samb*V*ca package.[18]

## 3. Results and Discussion

***3.1. GRIM initiation mechanism***: Treatment of 2,5-dibromo-3-butylthiophene monomer, **1**, with one equivalent of an alkyl or vinyl Grignard reagent results in a magnesium-bromine exchange reaction (**Scheme 2**), also referred to as Grignard metathesis. This reaction leads to two regiochemical isomers, **I1** and **I2**. Energy results showed that they are nearly isoenergetic, being **I1** is only 0.1 kcal·mol$^{-1}$ more stable than **I2**. From an energy point of view, this reaction proceeds by a low degree of regioselectivity, thus, for selective synthesis of either **I1** or **I2**, other parameters like the bulkiness of Grignard reagent should be considered.

It is assumed that GRIM polymerization proceeds by a transition metal-catalyzed cross-coupling reaction of **I1** or **I2** with a suitable catalyst. The Ni(II) and Pd(II) complexes including the dppp ligand were among the first examples of GRIM catalysts capable of coupling either **I1** or **I2** active monomers to produce high molecular weight polymers.[5] Experimental results showed that changes in the transition metal type can potentially control the properties of the resulting

polymer, including their stereoregularity.[5] Therefore, it is important to understand how changes of the catalyst type affect the elementary reactions of the polymerization process. Here, we will discuss the effect of the transition metal, Pd and Ni, on the regioselectivity of GRIM type coupling reaction when dppp used as ligand.

The mechanism of polymerization with these catalysts involves three main catalytic steps: oxidative addition, transmetalation, and reductive elimination, which will be studied in the present work in more detail.

Focusing first on the initiation step, initiators for GRIM polymerization are formed via two-step transmetalation involving 1 equiv of catalyst and 2 equiv of either **I1** or **I2** active monomers. Also, it is believed that upon addition of catalyst the regioisomer **I1** is only incorporated into the polymer while the more sterically hindered **I2** is not consumed during the polymerization,[19] however, it was uncertain what exactly makes the **I2** to be unreactive under GRIM polymerization conditions and no correct understanding of this process exists at this moment. So, we decided to study transmetalation of **I2**, as well.

Energy profiles for the main phases of coupling reaction using Ni(dppp)$Cl_2$ and Pd(dppp)$Cl_2$ catalysts are sketched on Fig 1 and Fig 2 and the numeric data are collected on Table 1 and Table 2. The first transmetalation of **I1** and **I2** gives rise to the formation of **COO1** and **COO2** intermediates, respectively (see Schemes 4 and 5). This reaction is barrierless and lead to 8.0 and 4.0 kcal·mol$^{-1}$ energy gain, when using Ni(dppp)$Cl_2$ as a catalyst, for the corresponding **COO1** and **COO2** intermediates, respectively, indicative of an already reasonable interaction between the Ni and two intermediates. Less stability of **COO2** can be attributed to the more sterically-demanding effect of butyl chain in **I2**.

**Table 1.** Relative energies (kcal·mol$^{-1}$) of stationary points on the potential energy surfaces (PES) of monomer couplings via Ni(dppp)$Cl_2$ catalyst

| Ni(dppp)$Cl_2$ | $E_{1stCOO}$ | $E_{2ndCOO}$ | $E_{TS}$ | $E_{act}$[a] | $E_{product}$ |
|---|---|---|---|---|---|
| Monomer **1**- Monomer **1** (t) | -8.0 | -11.1 | 1.2 | 12.3 | -24.5 |
| Monomer **1**- Monomer **1** (s) | -8.0 | -9.0 | 5.0 | 14.0 | -22.6 |
| Monomer **1**- Monomer **2** (t) | -8.0 | -8.7 | 5.5 | 14.2 | -22.0 |
| Monomer **1**- Monomer **2** (s) | -8.0 | -7.2 | 7.3 | 14.6 | -21.3 |
| Monomer **2**- Monomer **2** (t) | -4.0 | -5.6 | 9.5 | 15.1 | -17.2 |
| Monomer **2**- Monomer **2** (s) | -4.0 | -4.9 | 10.7 | 15.6 | -16.5 |

[a] Insertion barrier

Further, by changing transition metal from Ni to Pd, the first transmetalation becomes even energetically more facile, leading to an energy gain of 9.8 and 5.9 kcal·mol$^{-1}$ for the corresponding **COO1** and **COO2** intermediates, respectively.

**Table 2.** Relative energies (kcal·mol$^{-1}$) of stationary points on the potential energy surfaces (PES) of monomer couplings via Pd(dppp)$Cl_2$ catalyst

| $Pd(dppp)Cl_2$ | $E_{1stCOO}$ | $E_{2ndCOO}$ | $E_{TS}$ | $E_{act}$ [a] | $E_{product}$ |
|---|---|---|---|---|---|
| Monomer **1**- Monomer **1** (t) | -9.8 | -14.0 | 1.3 | 15.4 | -29.0 |
| Monomer **1**- Monomer **1** (s) | -9.8 | -12.1 | 4.3 | 16.4 | -27.0 |
| Monomer **1**- Monomer **2** (t) | -9.8 | -11.8 | 5.0 | 16.8 | -26.9 |
| Monomer **1**- Monomer **2** (s) | -9.8 | -10.8 | 6.3 | 17.2 | -25.8 |
| Monomer **2**- Monomer **2** (t) | -5.9 | -10.1 | 7.4 | 17.5 | -23.4 |
| Monomer **2**- Monomer **2** (s) | -5.9 | -9.1 | 9.0 | 18.1 | -23.1 |

[a] Insertion barrier

Since there are two isomeric active monomers in the mixture, in the second transmetalation stage, three isomeric intermediates, namely **COO11** (**I1-I1** coordination), **COO12** (**I1-I2** coordination) and **COO22** (**I2-I2** coordination), could in principle be formed and in each intermediate thiophene rings can be in the syn or anti position, thus doubling the number of isomeric intermediates to be considered as depicted in Schemes 4 and 5. Anti and syn structures were specified by (t) and (s) letters followed by the name of each intermediate, respectively. For example **COO11(t)** and **COO11(s)** refer to the coordination of two **I1** into the catalyst, in which thiophene rings are located in the anti and syn position, respectively. As seen, syn and anti forms differ only in the arrangement of the active monomer in coordination with Ni catalyst.

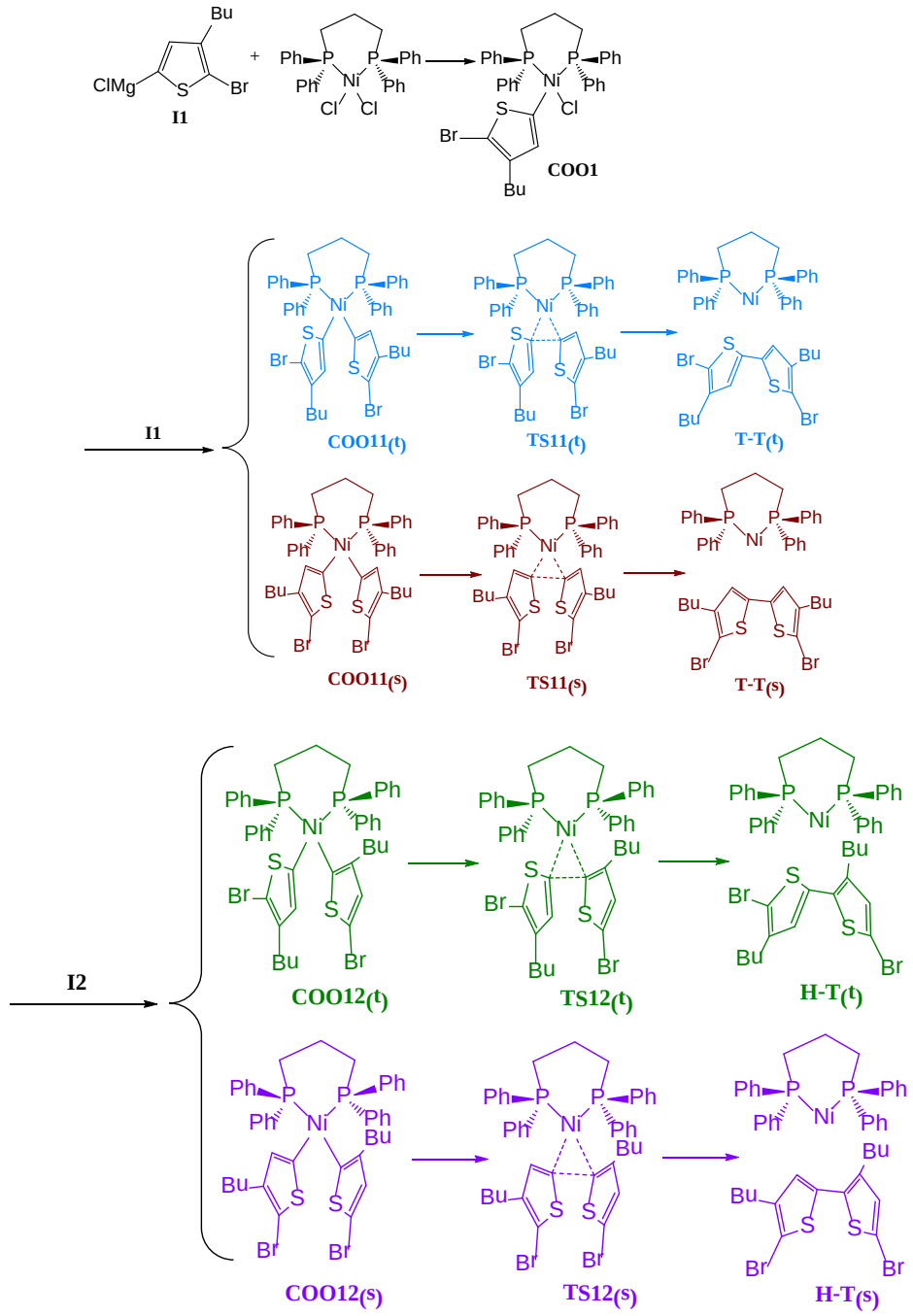


**Scheme 4**

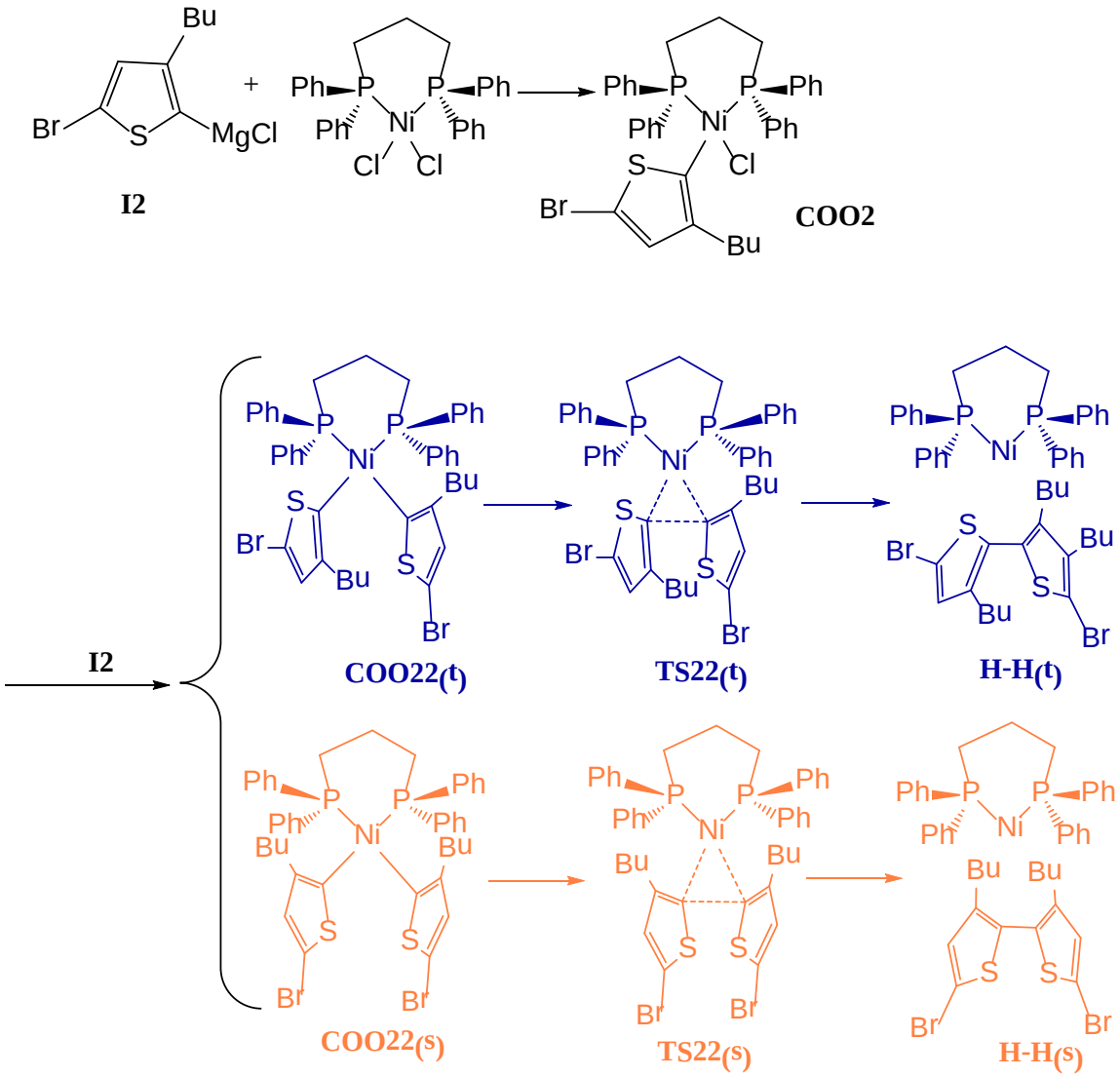


**Scheme 5**

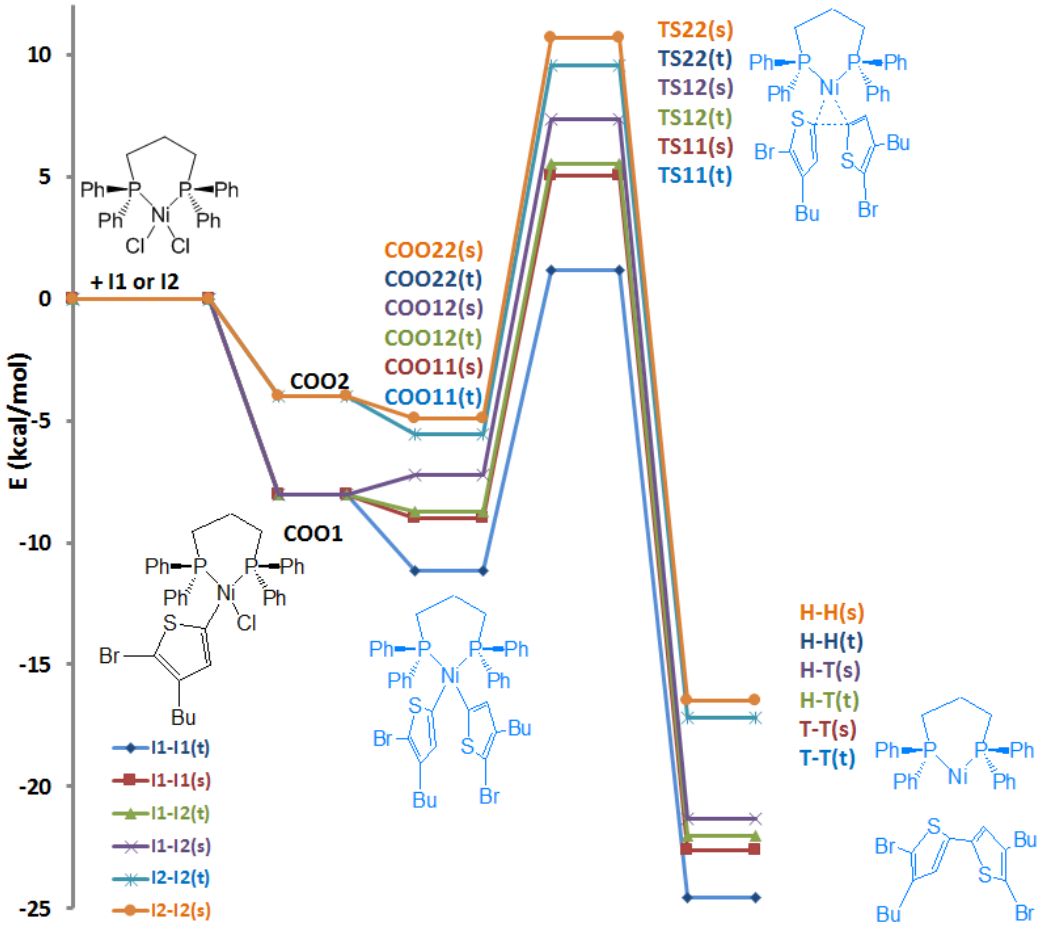


Fig 1. Relative energy profile for the first monomers coupling via Ni(dppp)$Cl_2$ catalyst.

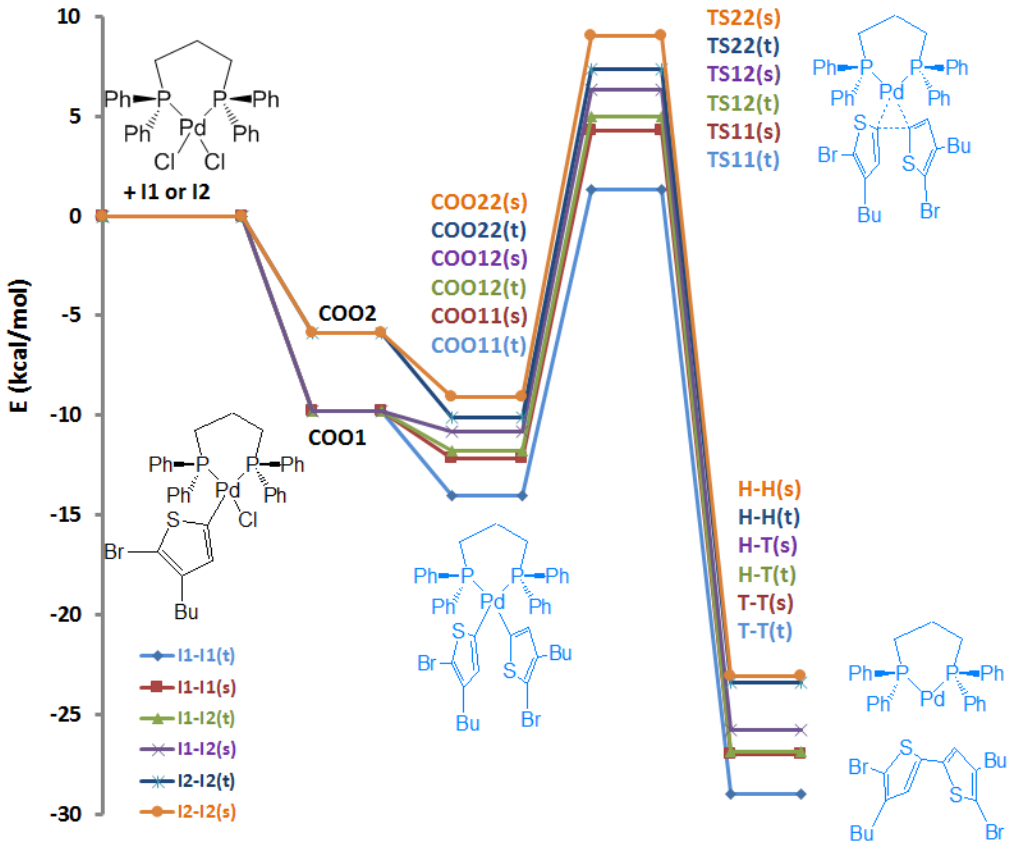


Fig 2. Relative energy profile for the first monomers coupling via Pd(dppp)$Cl_2$ catalyst.

Energy results in Table 1 indicate that all six secondary transmetalation reactions were also exoergonic. Generally, the (t) forms were more stable than the (s) forms and among the all secondary transmetalation reactions, **COO11(t)** had the highest energy gain of 11.1 kcal·mol$^{-1}$ due to the less steric effects between two thiophene rings. On the other hand, **COO22(s)** showed the lowest energy gain of 4.9 kcal·mol$^{-1}$ due to the higher steric effects of bulky butyl chains, which were closely located towards each other in the syn position, causing repulsion. It is interesting to note that, **COO11(s)** intermediate showed the second most stable form among all

other structures, indicating more chances of this coordination mode in comparison with **I1-I2** and **I2-I2** coordination pairs.

Moving to second transmetalation step accomplished by Pd(dppp)$Cl_2$ catalyst, in line with the results obtained for the second transmetalation by Ni catalyst, there is a regular increasing trend from -14.0, to -12.1, -11.8, -10.8, -10.1, and -9.1 kcal·mol$^{-1}$ for the series including **COO11(t)** to **COO11(s)**, **COO12(t)**, **COO12(s)**, **COO22(t)** and **COO22(s)**, respectively. This increase in the transmetalation energy can be attributed to the higher steric effect in the syn form, especially when **I2** is involved.

These results indicate that the nickel catalyst can differentiate the **COO11(t)** from the other intermediates with an energy difference ranging from 2.2 to 6.2 kcal·mol$^{-1}$ higher than the palladium catalyst, for which the energy difference was calculated from 1.9 to 4.9 kcal·mol$^{-1}$.

In the next step, the coupling of coordinated thiophene monomers occurs through a ring structured transition state **TS**, see Scheme 4 and Scheme 5, at 12.3, 14.0, 14.2, 14.6, 15.1, and 15.6 kcal·mol$^{-1}$ when used Ni catalyst and at 15.4, 16.4, 16.8, 17.2, 17.5 and 18.1 kcal·mol$^{-1}$ when used Pd catalyst, above **COO11(t)**, **COO11(s)**, **COO12(t)**, **COO12(s)**, **COO22(t)**, and **COO22(s)**, respectively. Using these data, it is possible to assess the preference for the particular mode of coupling by considering $E_{act}$ of the reaction. For the cases analyzed within this work, the upper barrier is due to the T-T(t) formation, being the lowest insertion barrier 12.3 and 15.4 kcal·mol$^{-1}$ for Ni and Pd catalysts, respectively.

Finally, reductive elimination from the **COO** intermediates occurs immediately to form an associated pair and a Ni(0) or Pd(0) organometallic compound. The pathway we considered is shown in Scheme 4 and Scheme 5. This reaction thermodynamically favored, with an energy

gain of 16.5-24.5 kcal·mol$^{-1}$ in the case of Ni catalyst, and 23.1-29.0 kcal·mol$^{-1}$ for the Pd catalyst, demonstrating the feasibility of this coupling reaction.

It was before suggested that a coupling reaction, which motives chain propagation, is prohibited if the transmetalation step would lead to sterically hindered head-to-head (HH) intermediates, i.e. **COO22(t)** and **COO22(s)**, in which alkyl substituents at both thienyl rings are in the "ortho" position relative to the metal center. However, reaction proceeds if no alkyl substituents are present at least at one "ortho" position relative to the Ni center.[20] Our calculations agree with such hypothesis and show that although the reaction is favorable thermodynamically when **H-H(t)** and **H-H(s)** are produced as well, the activation energy which should be overcome in **TS22(t)** and **TS22(s)** has much larger values among all other transition barriers.

It means that insertion of monomer **2** starting from both the **COO1** and **COO2** intermediates requires larger activation energy than that of monomer **1**. The higher barrier for monomer **2** insertion is due to the fact that complexes containing monomer **2**, **COO12(t)**, **COO12(s)**, **COO22(t)** and **COO22(s)**, have less stabilization energy than the ones only containing monomer **1**, **COO11(t)** and **COO11(s)**. Moreover, transition states **TS12(t)**, **TS12(s)**, **TS22(t)** and **TS22(s)** are less stable than **TS11(t)** and **TS11(s)**. This is mainly due to the more favourable electrostatic attraction and less serious exchange repulsion in structures containing intermediate **2**. On the other hand, in **TS22(t)** and **TS22(s)** structures the butyl groups of monomer **2** are closely located to each other, causing an exchange repulsion. From this section it can be concluded that the insertion of monomer **2** was more difficult than that of monomer **1**, due to the higher $E_{act}$. These theoretical results are in good qualitative agreement with the experimental observations which show more reactivity of monomer **1** in the polymerization process.[21]

From this section it is concluded that while the reaction mechanisms involving Ni(dppp)$Cl_2$ have been found to be similar to those with Pd(dppp)$Cl_2$, the nickel catalyst is found to differentiate from the other products the **H-H(t)** product, which is thermodynamically and kinetically the most favorable one among all products, more than the palladium catalyst can do. It means that for the Ni(dppp)$Cl_2$ catalyst, the **COO11(t)** isomer and the corresponding **T-T(t)** product are more stable than the other isomers and products to a greater extent than Pd(dppp)$Cl_2$, so that the coupling of monomer **1**-monomer **1** in trans form is relatively more favored for Ni(dppp)$Cl_2$ than for Pd(dppp)$Cl_2$. Our computational approach reproduces well the experimentally obtained higher stereospecifity of the P3ATs synthesized by Ni(dppp)$Cl_2$ relative to that synthesized by Pd(dppp)$Cl_2$ catalyst (98% vs 87%).[5] Indeed, Stefan et al were recently found that in a remarkable contrast to the nickel mediated reaction, polymerization with Pd(dppe)$Cl_2$ catalyst consumes both isomers **I1** and **I2** which results in a lower regioselectivity of Pd catalyst.[22] This finding is also in a good agreement with our obtained results.

***3.2. Chain Growth Mechanism***: After exploring all the initiation modes, we now proceed to study the chain growth mechanism considering newly formed associated pairs, Ni(0) active catalyst and unreacted **I1** and **I2** active monomers which are present in the reaction medium. In nickel catalyst, the chain-growth mechanism is provided by the fact that the Ni(0) catalytic species eliminated upon the reductive elimination step do not dissociates from the growing chains, but instead forms complexes with them and undergoes intramolecular oxidative addition into the C-Br bond present in the same chains.[20] This should result in selective oxidative addition of the polymer propagating end to the Ni(0) catalyst and a chain-growth polymerization.[1] By contrast, palladium dissociates from the growing chain and proceeds polymerization via a step growth mechanism.[22] Progress of the reaction by Pd catalyst has been carefully investigated by

other authors,[22] so we will discuss here the progress of the reaction using Ni catalyst. Before, it was shown that nickel can involve in transfer/diffusion from chain to chain during polymerization. Transfer of nickel usually occurs from higher molecular weight chains to both monomers and the oligomer.[23] In the case of transfer to monomers, reaction proceeds via the similar mechanism which was explained in *GRIM initiation* section. However, transfer to the oligomer has the same mechanism as intramolecular oxidative addition which will be discussed here.

To simulate the progress of the reaction we considered only **T-T(t)** + Ni(0) as active species, since we have shown in the previous section that this is the dominant species that can exist in the initial stages of the polymerization. By intramolecular oxidative addition of C-Br of **T-T(t)** bond to the Ni(0) centre, new organonickel compound, **COO3**, is generated in view of the fact that the formation of the complex **COO3** eliminates potential separation of **T-T (t)** from Ni(0) center. The energy profile for the formation of **COO3** from the starting Ni(0) ⋯ **T-T(t)** species is shown in Table 3 and Fig 3. Coordination of **T-T(t)** to the Ni(0) center, leading to **COO3** intermediates, is favoured by 32.6 kcal·mol$^{-1}$. When **I1** and **I2** active monomers coordinate to **COO3**, four different isomers can be obtained, shown in Scheme 6, which can be distinguished as **COO31(t)**, **COO31(s)**, **COO32(t)**, and **COO32(s)**.

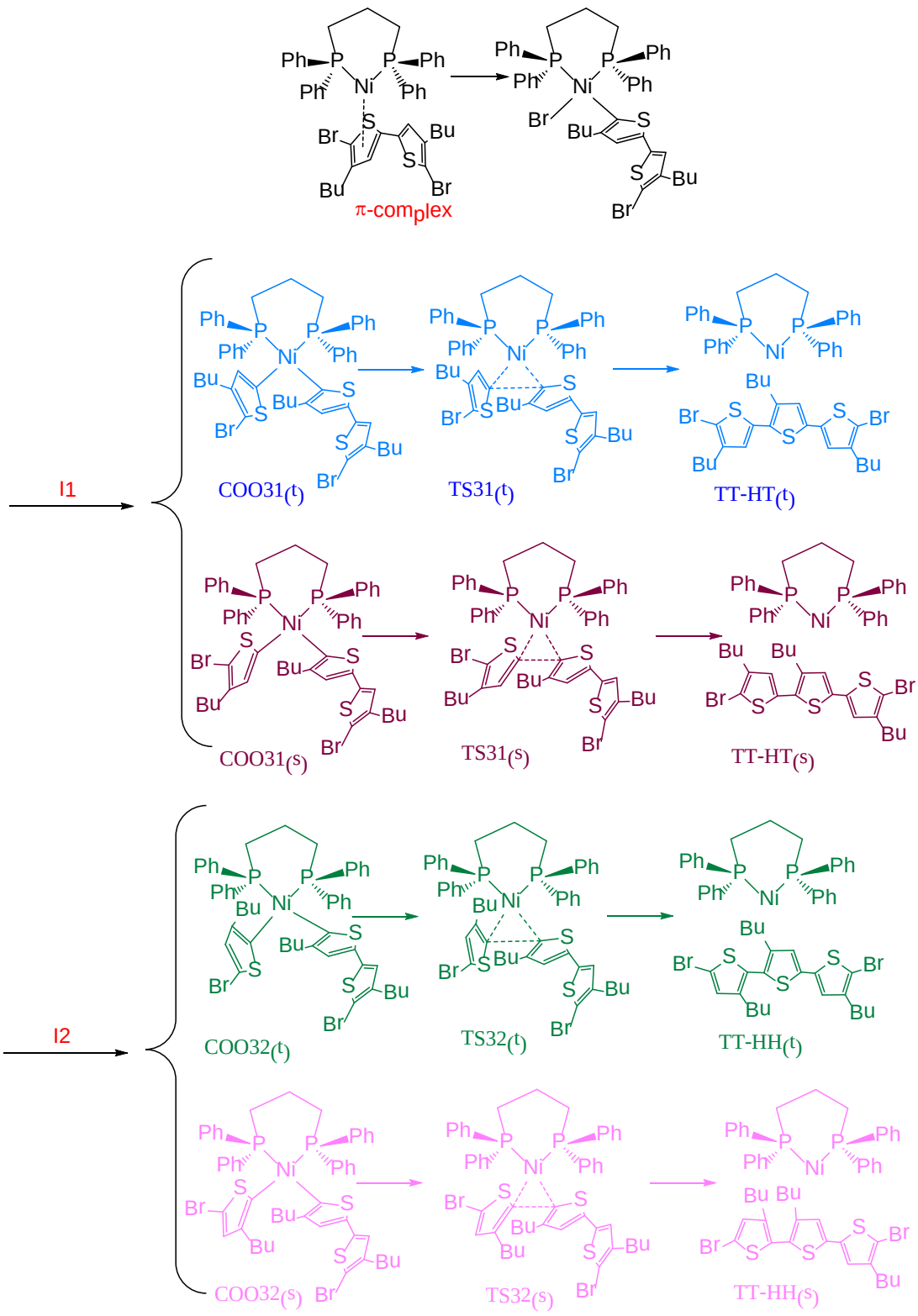


**Scheme 6.**

After geometry optimization it was found that **COO31(t)**, which is located at 37.6 kcal·mol$^{-1}$ below the starting material, is lower in energy than **COO31(s)**, **COO32(t)**, and **COO32(s)** by 1.6, 2.5 and 4.0 kcal·mol$^{-1}$, respectively.

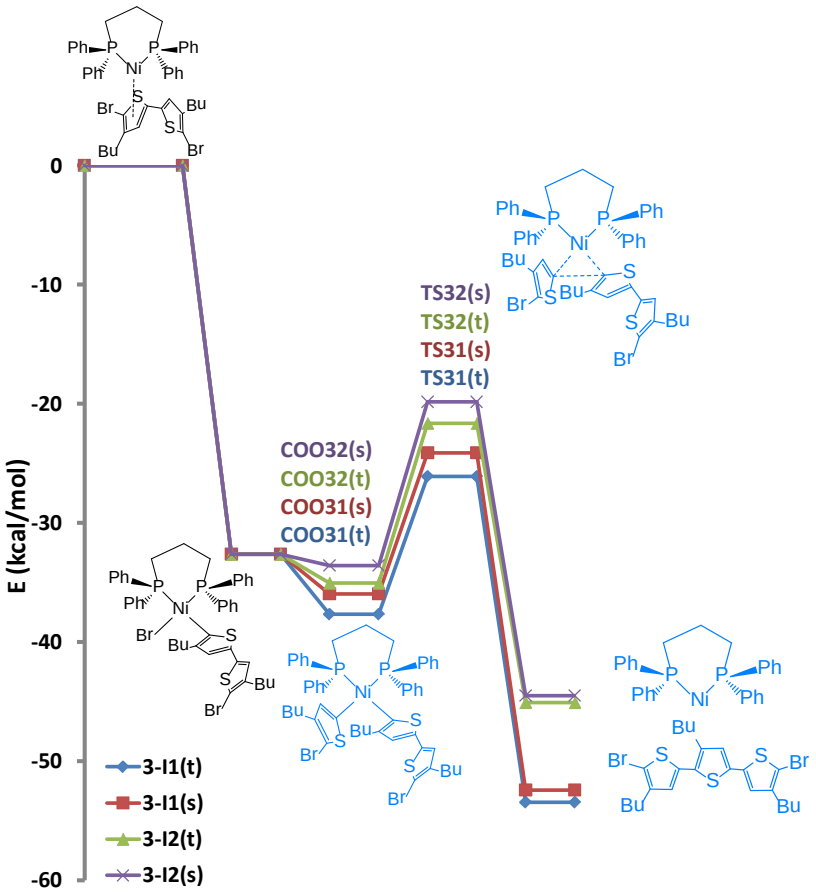


Fig 3. Relative energy profile for the chain growth mechanism via Ni(dppp)$Cl_2$ catalyst

**Table 3.** Relative energies (kcal·mol$^{-1}$) of stationary points on the potential energy surfaces (PES) of Pr-1 with **I1** and **I2** couplings via Ni(dppp)$Cl_2$ catalyst

| | | $E_{1stCOO}$ | $E_{2ndCOO}$ | $E_{TS}$ | $E_{act}$[a] | $E_{product}$ |
|---|---|---|---|---|---|---|
| T-T(t) | **I1(t)** | -32.6 | -37.6 | -26.1 | 11.5 | -53.4 |
| | **I1(s)** | -32.6 | -36.0 | -24.1 | 11.9 | -52.4 |
| | **I2(t)** | -32.6 | -35.1 | -21.6 | 13.5 | -45.1 |
| | **I2(s)** | -32.6 | -33.6 | -19.8 | 13.8 | -44.5 |

[a] Insertion barrier After this transmetalation, the monomers move further beyond the Metal-C bond so that the reaction passes through a three-membered ring structure containing C-Metal-C atoms, and the energy rises to reach the transition state. A barrier of 11.5-13.8 kcal·mol$^{-1}$ has to be overcome in order to couple coordinated monomers. Finally, the transition state structures collapse into the corresponding Ni(0) ···· trimer complex, at 53.4-44.5 kcal·mol$^{-1}$ below the starting materials.

Based on these calculations, the conclusion emerging from the energy values given in Table 3 is that, in the framework of the studied mechanism, the key step determining the experimentally observed preferential formation of *trans*-isomers is the **COO3** to **COO3n** step. Free and fast rotation around the metal-thiophene bond allows the thermodynamically more stable oxidative addition isomer, i.e. **COO3n(t)**, to be generated in higher yields.

### *3.3. Catalyst Maps*

To analyse the steric influence of the dppp ligand we used topographic steric maps (Fig 4). The points in space defining the steric map were located with the SambVca package developed by Cavallo et al.[18] This program analyzes the first coordination sphere around the metal, which is the place where catalysis occurs. It is normally used to calculate the buried volume of a given ligand, which is a number that quantifies the amount of the first coordination sphere of the metal occupied by this ligand.[24-26] A modified version of SambVca allows the user to perform a more detailed analysis by evaluating the $\%V_{Bur}$ in the single quadrants around the metal center. Splitting the total $\%V_{Bur}$ into quadrant contributions quantifies any asymmetry in the way the ligand wraps around the metal and allows one to understand how changing the ligand from dppe to dppp modifies the shape of the reactive pocket.[24,27,28]

$\%\ V_{Bur}$ values (see Table 4), obtained by analysing the steric bulk of the dppp ligand in the DFT optimized structure of the Ni(dppp)$Cl_2$ and Pd(dppp)$Cl_2$ complexes. The data reported in Table 4 indicate that dppp ligand in Ni(dppp)$Cl_2$ catalyst shows a $\%V_{Bur}$ slightly higher than that of the Pd(dppp)$Cl_2$ analogue which can be the origin of selectivity in this catalyst.

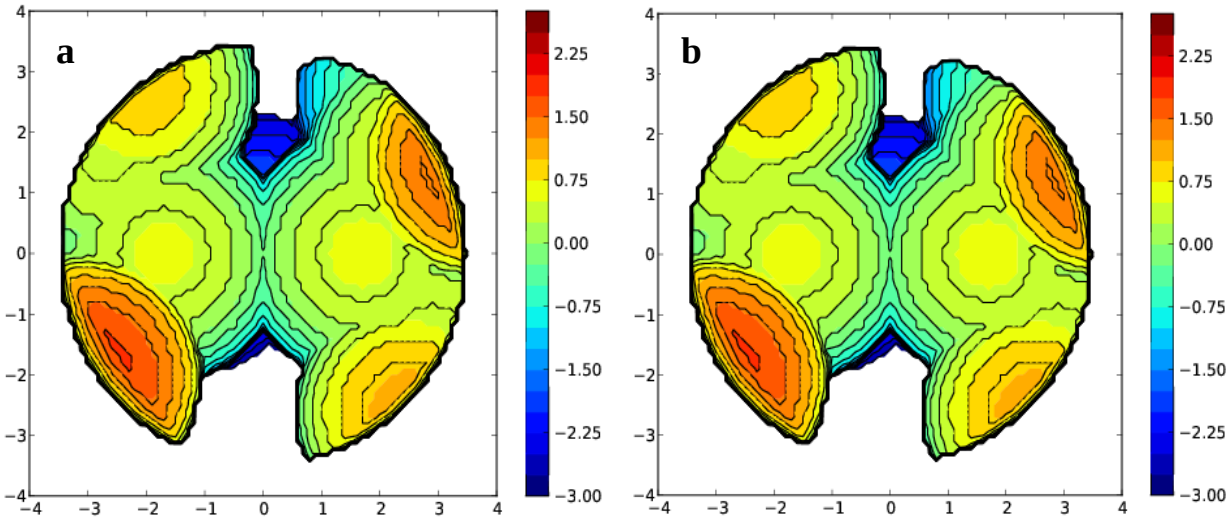


Fig 4. %*V*Bur maps of the dppp ligand in the optimized geometries of (a) Ni(dppp)$Cl_2$, (b) Pd(dppp)$Cl_2$ complexes.

Table 4. %$V_{Bur}$ Values for Ni(dppp)$Cl_2$, Pd(dppp)$Cl_2$, and Ni(PPh3)$_2Cl_2$ catalysts.

| | **%$V_{Bur}$** | **Regioregularity H-T(%)** | **Ref** |
|---|---|---|---|
| Ni(dppp)$Cl_2$ | 53.2 | 98 | [5] |
| Pd(dppp)$Cl_2$ | 52.1 | 87 | [5] |

## Conclusion

DFT calculations have been employed to explore the mechanism of polymerization of 2,5-dibromo 3-butylthiophene monomer via Grignard metathesis polymerization mechanism using commonly used catalysts including Ni(dppp)$Cl_2$, and Pd(dppp)$Cl_2$. Results indicated that all primary and secondary transmetalation reactions including **I1-I1(t)**, **I1-I1(s)**, **I1-I2(t)**, **I1-I2(s)**, **I2-I2(t)**, and **I2-I2(s)** coordination with both Ni(dppp) and Pd(dppp) catalysts were favoured with respect to separated species. Further, our calculations suggest that the origin of the preferential formation of tail isomers is due to the coordination step, which prevents the initially formed COO-nn(s) from proceeding of the reaction, and returns it to the reaction pool until the

COO-nn(t) is formed. Also, we found that both kinetic (low energy barrier, $E_{act}$) and thermodynamic (low energy product) arguments based on catalyst selectivity can support the origin of HT regioselectivity, and better selectivity, with lower $E_{act}$ and larger $\Delta E_{act}$, was achieved when Ni(dppp)$Cl_2$ used as a catalyst. % $V_{Bur}$ values, of the Ni(dppp)$Cl_2$ and Pd(dppp)$Cl_2$ complexes indicate that dppp ligand in Ni(dppp)$Cl_2$ catalyst shows a %$V_{Bur}$ slightly higher than that of the Pd(dppp)$Cl_2$ analogue, which can be the origin of higher selectivity in this catalyst.

**Acknowledgements**

This work has been supported by Iran's National Foundation of Elites. The authors thank MOLNAC (www.molnac.unisa.it) for its computer facilities and also the SambVca online service (http://www.molnac.unisa.it/OMtools/sambvca.php) for computing %$V_{Bur}$. A.P. thanks the Spanish MINECO for a Ramón y Cajal contract (RYC-2009-05226) and European Commission for a Career Integration Grant (CIG09-GA-2011-293900).

**Supporting Information**. Cartesian coordinates and energies in a.u. of all the species discussed in the text are available free of charge via the Internet at http://www.rsc.org.

## References


1. A. Yokoyama, R. Miyakoshi and T. Yokozawa, *Macromolecules*, 2004, **37**, 1169-1171.
2. S. Savagatrup, A. D. Printz, D. Rodriquez and D. J. Lipomi, *Macromolecules*, 2014, **47**, 1981-1992.
3. Z. Hu, T. Adachi, Y.-G. Lee, R. T. Haws, B. Hanson, R. J. Ono, C. W. Bielawski, V. Ganesan, P. J. Rossky and D. A. Vanden Bout, *ChemPhysChem*, 2013, **14**, 4143-4148.
4. L. A. Perez, P. Zalar, L. Ying, K. Schmidt, M. F. Toney, T.-Q. Nguyen, G. C. Bazan and E. J. Kramer, *Macromolecules*, 2014, **47**, 1403-1410.
5. Y. Mao, Y. Wang and B. L. Lucht, *Journal of Polymer Science Part A: Polymer Chemistry*, 2004, **42**, 5538-5547.
6. C. Bruner and R. Dauskardt, *Macromolecules*, 2014, **47**, 1117-1121.
7. J.-M. Jiang, H.-K. Lin, Y.-C. Lin, H.-C. Chen, S.-C. Lan, C.-K. Chang and K.-H. Wei, *Macromolecules*, 2014, **47**, 70-78.
8. R. D. McCullough, *Adv. Mater.*, 1998, **10**, 93-116.
9. R. D. McCullough and R. D. Lowe, *J. Chem. Soc. Chem. Commun.*, 1992, 70-72.
10. T. A. Chen and R. D. Rieke, *J. Am. Chem. Soc.*, 1992, **114** 10087-10088.
11. I. Osaka and R. D. McCullough, *Acc. Chem. Res.*, 2008, **41** 1202-1214.
12. R. S. Loewe, P. C. Ewbank, J. Liu, L. Zhai and R. D. McCullough, *Macromolecules.*, 2001, **34**, 4324-4333.
13. M. J. Frisch, G. W. Trucks, H. B. Schlegel, G. E. Scuseria, M. A. Robb, J. R. Cheeseman, J. Montgomery, J. A., T. Vreven, K. N. Kudin, J. C. Burant, J. M. Millam, S. S. Iyengar, J. Tomasi, V. Barone, B. Mennucci, M. Cossi, G. Scalmani, N. Rega, G. A. Petersson, H. Nakatsuji, M. Hada, M. Ehara, K. Toyota, R. Fukuda, J. Hasegawa, M. Ishida, T.

Nakajima, Y. Honda, O. Kitao, H. Nakai, M. Klene, X. Li, J. E. Knox, H. P. Hratchian, J. B. Cross, C. Adamo, J. Jaramillo, R. Gomperts, R. E. Stratmann, O. Yazyev, A. J. Austin, R. Cammi, C. Pomelli, J. W. Ochterski, P. Y. Ayala, K. Morokuma, G. A. Voth, P. Salvador, J. J. Dannenberg, V. G. Zakrzewski, S. Dapprich, A. D. Daniels, M. C. Strain, O. Farkas, D. K. Malick, A. D. Rabuck, K. Raghavachari, J. B. Foresman, J. V. Ortiz, Q. Cui, A. G. Baboul, S. Clifford, J. Cioslowski, B. B. Stefanov, G. Liu, A. Liashenko, P. Piskorz, I. Komaromi, R. L. Martin, D. J. Fox, T. Keith, M. A. Al-Laham, C. Y. Peng, A. Nanayakkara, M. Challacombe, P. M. W. Gill, B. Johnson, W. Chen, M. W. Wong, C. Gonzalez and J. A. Pople, Gaussian, Inc., Pittsburgh PA,, Editon edn., 2003.

14. C. Y. Lee, W.; Parr, R.G., *Phys. Rev. B*, 1988, **37**, 785-789.
15. A. D. Becke, *J. Chem. Phys.*, 1993, **98**, 1372-1377.
16. A. Schäfer, H. Horn and R. Ahlrichs, *J. Chem. Phys.*, 1992, **97**, 2571-2580.
17. W. Kuechle, M. Dolg, H. Stoll and H. Preuss, *J. Chem. Phys.*, 1994, **100**, 7535-7542.
18. A. Poater, B. Cosenza, A. Correa, S. Giudice, F. Ragone, V. Scarano and L. Cavallo, *Eur. J. Inorg. Chem.*, 2009, 1759-1765.
19. M. C. Iovu, E. E. Sheina, R. R. Gil and R. D. McCullough, *Macromolecules*, 2005, **38**, 8649-8656.
20. R. Tkachov, V. Senkovskyy, H. Komber and A. Kiriy, *Macromolecules*, 2011, **44**, 2006–2015.
21. D. W. Laird, R. S. Loewe, P. C. Ewbank, J. Liu, L. Zhai and R. D. McCullough, *Polym. Prepr.*, 2001, **42**, 556-557.
22. M. P. Bhatt, H. D. Magurudeniya, P. Sista, E. E. Sheina, M. Jeffries-El, B. G. Janesko, R. D. McCullough and M. C. Stefan, *J. Mater. Chem. A*, 2013, **1**, 12841-12849.

23. B. C. Achord and J. W. Rawlins, *Macromolecules*, 2009, **42**, 8634-8639.

24. J. Bosson, A. Poater, L. Cavallo and S. P. Nolan, *J. Am. C. Soc.*, 2010, **132**, 13146-13149.

25. A. Poater, F. Ragone, S. Giudice, C. Costabile, R. Dorta, S. P. Nolan and L. Cavallo, *Organometallics*, 2008, **27**, 2679-2681.

26. A. Poater, B. Cosenza, A. Correa, S. Giudice, F. Ragone, V. Scarano and L. Cavallo, *Eur. J. Inorg. Chem.*, 2009, **2009**, 1759-1766.

27. A. Poater, L. Falivene, C. A. Urbina-Blanco, S. Manzini, S. P. Nolan and L. Cavallo, *Dalton Trans.*, 2013, **42**, 7433-7439.

28. A. Poater, F. Ragone, R. Mariz, R. Dorta and L. Cavallo, *C. Eur. J.*, 2010, **16**, 14348-14353.

# Exploring the Mechanism of Grignard Methathesis Polymerization of 3-alkylthiophenes

**Naeimeh Bahri-Laleh[1]*, Albert Poater[2], Luigi Cavallo[3], Seyed Amin Mirmohammadi[1]**

[1] *Department of Polymerization Engineering, Iran Polymer and Petrochemical Institute, P.O. Box 14965/115, Tehran, Iran.* [2] *Institut de Química Computacional i Catàlisi and Departament de Química, Universitat de Girona, Campus Montilivi, 17071 Girona, Catalonia, Spain.* [3] *Department of Chemistry, University of Salerno, Via Ponte don Melillo, Fisciano I-84084, Italy.*

**To whom correspondence should be addressed**: n.bahri@ippi.ac.ir, Tel: +982148662339, Fax: +982144196583.